IEEE Access
Multidisciplinary ⋮ Rapid Review ⋮ Open Access Journal

Received 5 September 2022, accepted 21 September 2022, date of publication 26 September 2022,
date of current version 30 September 2022.

Digital Object Identifier 10.1109/ACCESS.2022.3209501

RESEARCH ARTICLE

Design and Analysis of Single Inverter-Fed Brushless Wound Rotor Vernier Machine

SARA TARIQ[1], JUNAID IKRAM[1], SYED SABIR HUSSAIN BUKHARI[2], (Senior Member, IEEE), QASIM ALI[2], (Member, IEEE), ASIF HUSSAIN[3], AND JONG-SUK RO[4,5]

[1]Department of Electrical and Computer Engineering, COMSATS University Islamabad, Islamabad 45550, Pakistan
[2]Department of Electrical Engineering, Sukkur IBA University, Sukkur, Sindh, Pakistan
[3]Department of Electrical Engineering, University of Management and Technology, Lahore 54770, Pakistan
[4]School of Electrical and Electronics Engineering, Chung-Ang University, Seoul 06910, South Korea
[5]Department of Intelligent Energy and Industry, Chung-Ang University, Seoul 06910, South Korea

Corresponding author: Jong-Suk Ro (jongsukro@gmail.com)

This work was supported in part by the National Research Foundation of Korea (NRF) Grant through the Ministry of Science and ICT under Grant NRF-2022R1A2C200487, and in part by the Brain Pool (BP) Program through the National Research Foundation (NRF) of Korea through the Ministry of Science and ICT under Grant 2019H1D3A1A01102988.

ABSTRACT In this paper, a brushless wound rotor vernier machine (Bl-WRVM) with a single inverter configuration is proposed to achieve the brushless operation. In the proposed topology, a single inverter is connected with series-connected ABC and XYZ windings through which the current flow produces the magnetomotive force with fundamental and sub-harmonic components, respectively. The XYZ windings have similar pole pairs to the excitation windings, whereas its number of poles is different from the ABC winding. A 24-slot stator, 4-pole armature ABC winding, 2 Pole armature XYZ and excitation windings, and 44-pole field winding for the outer rotor is designed and 2D finite element analysis is carried out to determine the performance of the machine. The proposed topology makes the Bl-WRVM cost-effective by applying only a single inverter as compared to a dual-inverter Bl-WRVM and it improves its torque quality.

INDEX TERMS Brushless, single-inverter-fed, harmonic field excitation, WRVMs.

I. INTRODUCTION

In recent years, the Permanent Magnet Vernier Machines (PMVMs) have gained a lot of interest due to their increasing demand in direct drive applications. PMVMs are capable of generating high torque at low speed due to the magnetic gearing effect as compared to the other types of PM machines. Furthermore, the mechanical gearing system which is noisy and costly can also be replaced with these machines. However, these machines suffer from speed controllability issues as speed rises, low power factor, and the high cost of the PMs [1], [2].

PMVMs are magnetically geared machines that have a magnetic gearing effect due to flux modulation. The earlier vernier reluctance machine is the base from which PMVMs are derived [3]. The output power achieved in PMVMs is three times to equivalent of conventional PM machines for a similar volume and current. Furthermore, PMVM is commonly designed for low-speed rotation due to a large number of magnet poles [4]. Because rare-earth permanent magnets are used in PMVMs, they are expensive as well [5]. PMVMs with dual-stator have auxiliary inner stator with no windings and the outer stator only comprise the windings. In this way torque density of the machine is improved because the whole volume of the structure is reduced. As a result, this machine will be lacking in manufacturing and thermal problems because this configuration does not have windings on the inner stator [6]. The hybrid excited PMVM was proposed in order to regulate flux in both directions, which have all of their excitation sources on the stator, thus it helps in regulating the temperature rise of magnets [7]. Axial flux PMVMs to improve power factor, and torque density and minimize the torque ripples by using spoke-type PM, notched-shaped PM and two-stage parallelogram-shaped PM were proposed

The associate editor coordinating the review of this manuscript and approving it for publication was Alfeu J. Sguarezi Filho.

in [8]. Although PMVMs generate very high torque but the issues associated with these machines are high-cost permanent magnets and their wide-speed operation.

Vernier reluctance machines (VRMs) are magnet-free machines and hence are less expensive as compared to the PMVMs. However, these machines suffer from low power factor and torque density as compared to PMVM. The stator-connected DC-VRM is also free from the PMs [9], [10], [11], [12]. Because of its high reliability, this machine is gaining more attention due to which it is being used in high-speed applications. However, as a consequence, the stator's armature and field windings limit the armature winding's fill factor and current density. By using a wound-rotor vernier machine, the field windings were placed on the rotary rotor instead of the stator. Furthermore, to keep the rotor excited, it is necessary to clean and maintain the brushes and slip-rings assemblies in this configuration [13].

In [10], a topology of a dual-inverter brushless wound-rotor machine (WRM) was presented to overcome the carbon brushes and slip ring issues by providing brushless excitation to the field winding. A rotating magnetomotive force (MMF) is generated from two inverters. This contains a fundamental and an additional subharmonic component for brushless rotor excitation. Brushes and slip-rings create the problem of sparking and require regular maintenance, but these issues are solved by brushless operation. However, its field winding is on the rotor, which avoids the issues of DC-VRM. In [14], a brushless wound-rotor vernier machine (BL-WRVM) was proposed for variable-speed applications. The speed of the machine was controlled by controlling the field flux. Moreover, the brushless topology avoids the problems of sparking and regular maintenance in rotor-current-excited vernier machines. In [15], a topology of the wound rotor machine with dual-mode was proposed. Dual mode operation was created by portioning the field winding into two groups to generate different rotor poles by changing field coils arrangements. In [16] a cost-effective scheme of brushless WRM is proposed by using a single inverter. This scheme uses a single inverter as opposed to a dual-inverter for the brushless operation of the WRM.

This paper presents a cost-effective single inverter-fed brushless wound rotor vernier machine having improved torque quality. The proposed stator winding is comprised of the four-pole and two-pole armature windings which are connected in series with each other. The main three-phase armature windings are named as ABC winding, whereas the additional three-phase armature winding is named as XYZ winding. The additional three-phase windings are responsible for the two-pole operation whereas the main three windings are responsible for the four-pole operation. When the current flows through these series-connected stator windings, the magnetomotive will be produced which has the fundamental and the subharmonic component.

The rest of the paper is organized as follows. In the second section, the conventional brushless WRVM [14] and the proposed WRVM configurations are discussed. In the third section, 2D finite element analysis (2D-FEA) simulation results for the conventional brushless WRVM and proposed brushless WRVM model are discussed. Finally, conclusions are drawn.

II. CONVENTIONAL DUAL-INVERTER BL-WRVM TOPOLOGY

In the conventional topology of the Bl-WRVM, the stator winding is spatially distributed into two equal parts to generate fundamental and subharmonic magnetomotive force. Both the stator windings (ABC and XYZ) are designed to generate the two four-pole armature windings. In order to generate subharmonic and fundamental magnetomotive forces, one armature winding is supplied with half of the current as opposed to the other half armature winding. Thus, the resultant armature magnetomotive force would have both the fundamental and subharmonics components. Figure 1 shows the schematic representation of the conventional dual-inverter Bl-WRVM. This is the brushless sub-harmonic topology introduced in [13] and also used for BL-WRVM in [14]. In this topology, 2 separate inverters supply currents to the distributed windings in the stator. The difference in magnitudes of currents from two inverters produces the subharmonic component of the MMF. This component of MMF is used for the rotor excitation, through the induction in excitation winding. The induced voltages are then fed to the rotating rectifier on the rotor converting it to DC current for the final use of field winding so that it produces the rotor field flux without the use of brushes and slip-rings.

The excitation winding of the conventional Bl-WRVM is comprised of the two-pole structure in order to link with the subharmonic component of the armature magnetomotive force. The voltage induced in the excitation winding is rectified with the help of the full-bridge rectifier in order to provide the excitation to the field winding. The field winding is comprised of a 44-pole concentrated winding arrangement in order to generate the vernier effect for the Bl-WRVM. Figure 2 shows the winding layout of the double-layer armature windings of the conventional dual-inverter Bl-WRVM. Both the armature windings have a coil span of 6 slots and is generating four poles. The winding coils are arranged in both forward and backward directions with the coils span of 6 for the ABC winding and 6 for the XYZ winding. The basic equation for the vernier operation is given by equation (1) as below.

$$P_r = Q_s - P_s \tag{1}$$

where P_r stands for the rotor pole pairs, Q_s represents the stator slots and P_s represents the stator pole pairs.

The currents supplied by inverter 1 to the stator winding ABC are given by the following equation.

$$\begin{aligned} I_A &= I\cos\omega_e t \\ I_B &= I\cos(\omega_e t - \frac{2\pi}{3}) \\ I_C &= I\cos(\omega_e t + \frac{2\pi}{3}) \end{aligned} \tag{2}$$

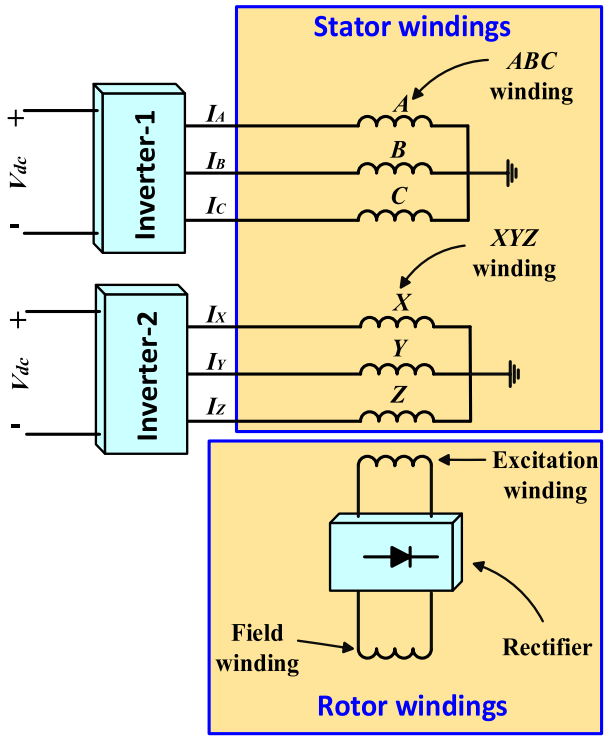

ABC winding: 4-pole; XYZ winding: 4-pole; Field winding: 44-pole; Excitation winding: 2-pole

FIGURE 1. Schematic diagram of conventional Bl-WRVM.

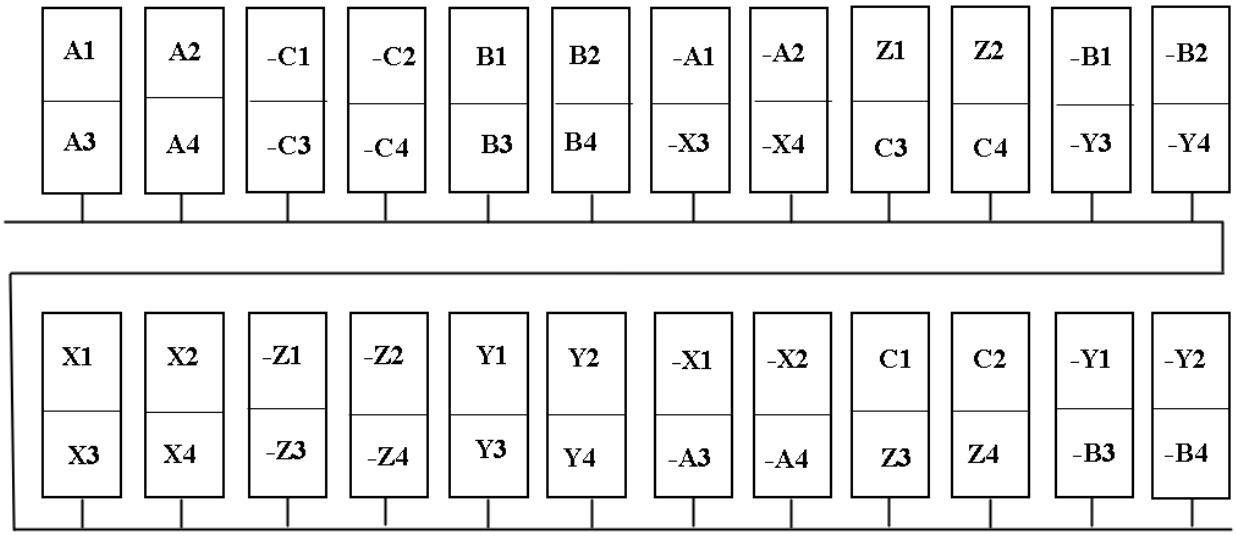

FIGURE 2. Conventional Bl-WRVM armature winding with coils wound in both forward and backward direction.

The currents supplied by inverter 2 to the stator winding XYZ are given by the following equation.

$$\begin{aligned} I_X &= \frac{1}{2} I \cos \omega_e t \\ I_Y &= \frac{1}{2} I \cos(\omega_e t - \frac{2\pi}{3}) \\ I_Z &= \frac{1}{2} I \cos(\omega_e t + \frac{2\pi}{3}) \end{aligned} \tag{3}$$

where I signify the current amplitude and ω_e denotes angular frequency.

III. PROPOSED SINGLE INVERTER BL-WRVM TOPOLOGY

In the proposed topology of Bl-WRVM, the stator winding is connected with a single inverter to generate a fundamental and subharmonic components of the magnetomotive force.

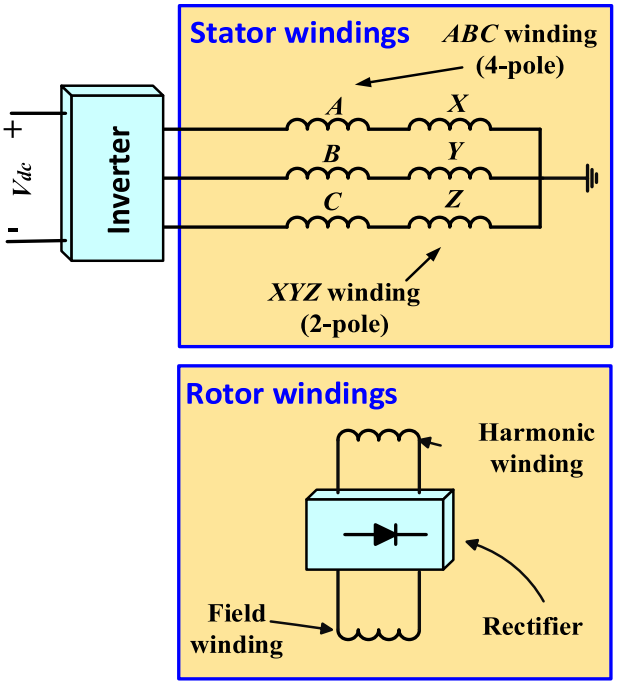

ABC winding: 4-pole; XYZ winding: 2-pole; Field winding: 44-pole; Excitation winding: 2-pole

FIGURE 3. Schematic diagram of proposed BI-WRVM.

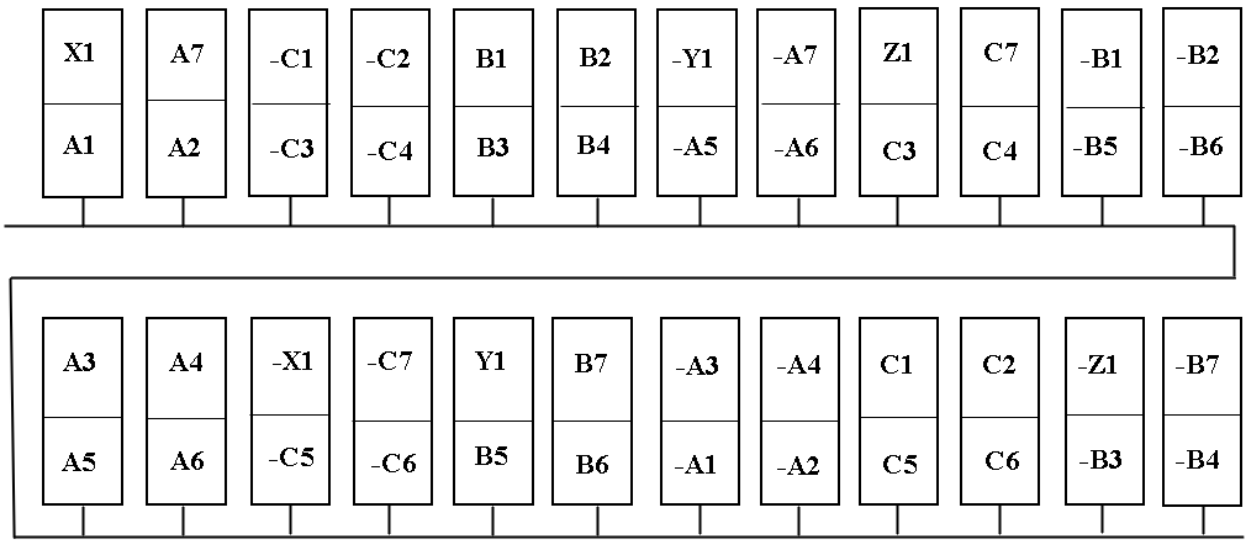

FIGURE 4. Proposed model design I with three slots for XYZ winding in forward backward arrangement.

The stator windings are comprised of the four-pole and two-pole armature windings which are connected in series with each other. The main three-phase armature windings are named as ABC winding, whereas the additional three-phase armature winding is named as XYZ winding. The additional three-phase windings are responsible for the two-pole operation whereas the main three windings are responsible for the four-pole operation. When the current flows through these series-connected stator windings, the magnetomotive will be produced which has the fundamental and the subharmonic component.

For the rotor configuration, two windings are employed named as excitation and field windings which are connected through a full-bridge rectifier. The full-bridge rectifier is

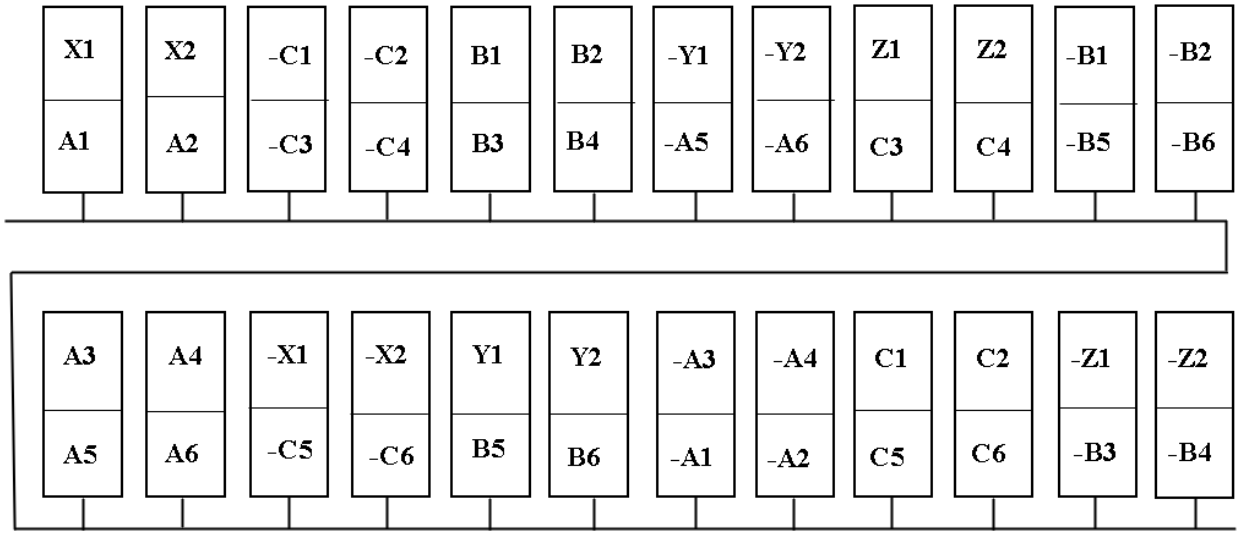

FIGURE 5. Proposed model design II with six slots for XYZ winding in forward backward arrangement.

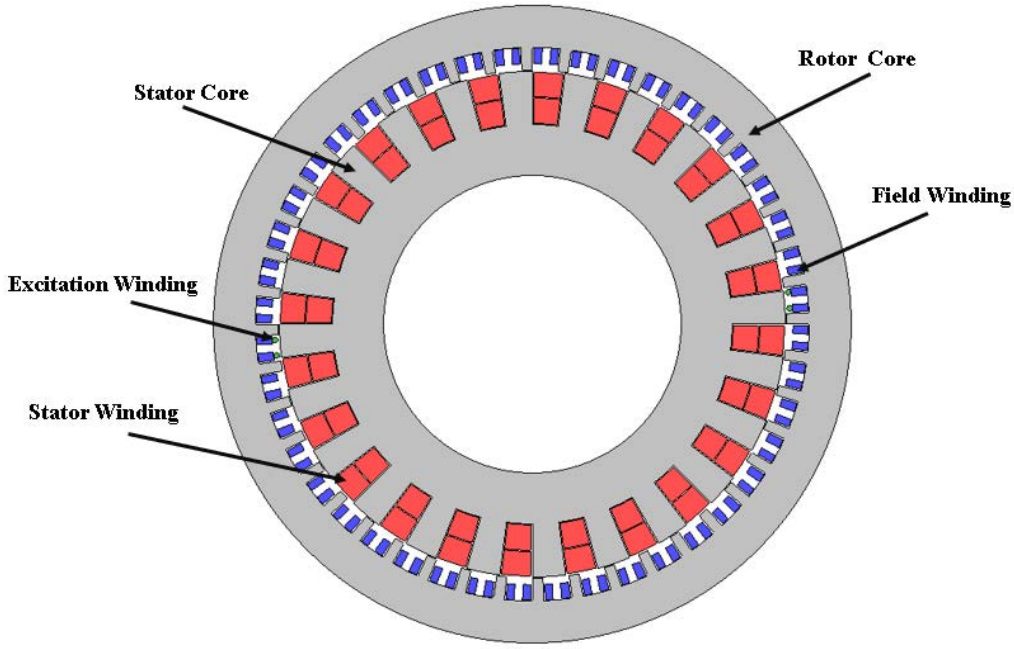

FIGURE 6. 2D model of the Bl-WRVM with its stator and rotor windings.

employed to convert the excitation winding induced voltage to the direct current voltage for the utilization of the field winding. The excitation winding is of two-pole configurations. The additional two pole armature winding when fed with the inverter causes the voltage to be induced on the two-pole excitation winding. The field winding is designed to produce 44 poles when fed with the dc current produced by the full-bridge rectifier. The 44 poles for the field winding are chosen to create the vernier operation of the brushless machine since the stator consists of 24 slots. The schematic representation of the proposed Bl-WRVM is shown in Fig. 3. In this topology, only a single inverter is used to supply currents to the distributed windings in the stator. Here one armature winding is a four-pole winding which is the main winding, while the other armature winding is a two-pole winding. The magnetomotive force of the two-pole armature winding induces the voltage into the two-pole excitation winding. The induced voltage of the harmonic winding is rectified with the help of the full-bridge converter to provide power to the excitation winding. Thus,

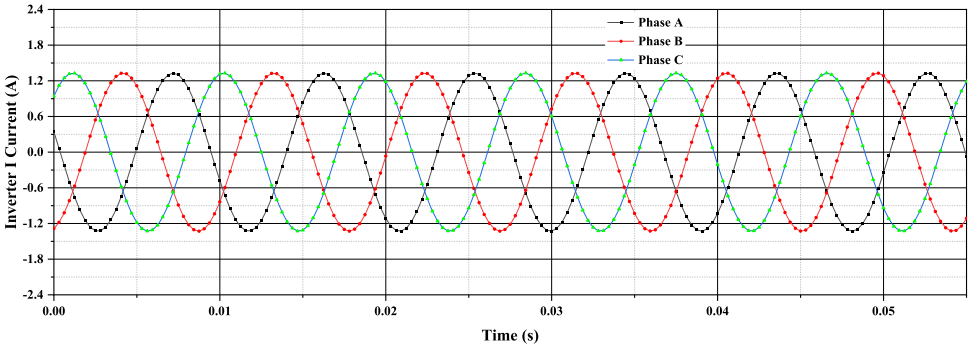

(a) Current fed by the Inverter I to the conventional model.

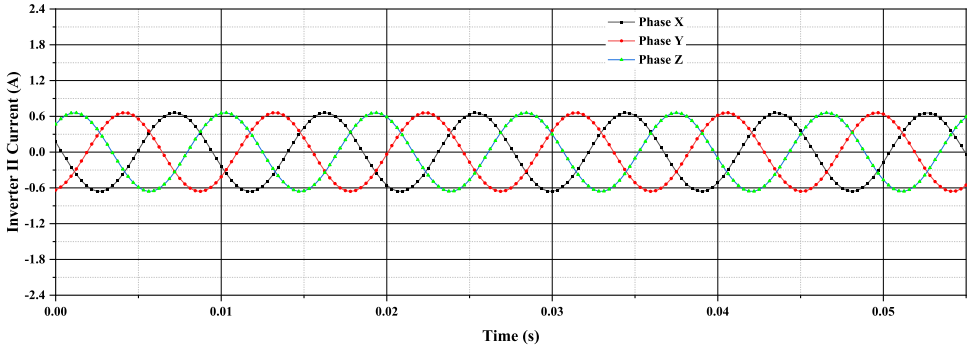

(b) Current fed by the inverter II to the conventional model.

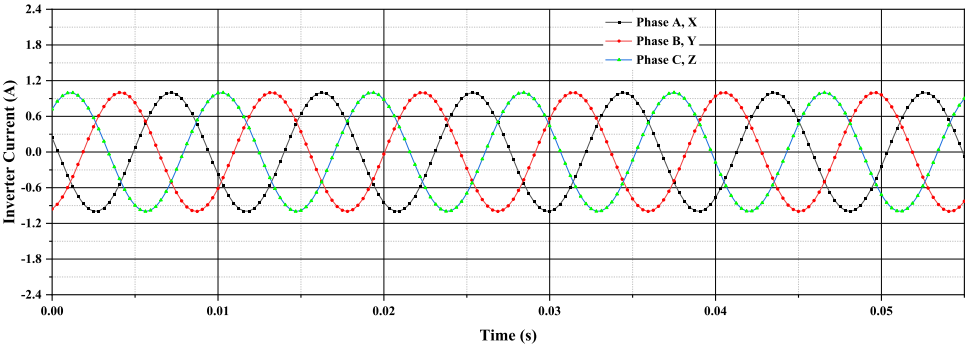

(c) Current fed by the inverter to the proposed model design I and II.

FIGURE 7. Current fed by the inverter to the conventional and proposed model design I and II.

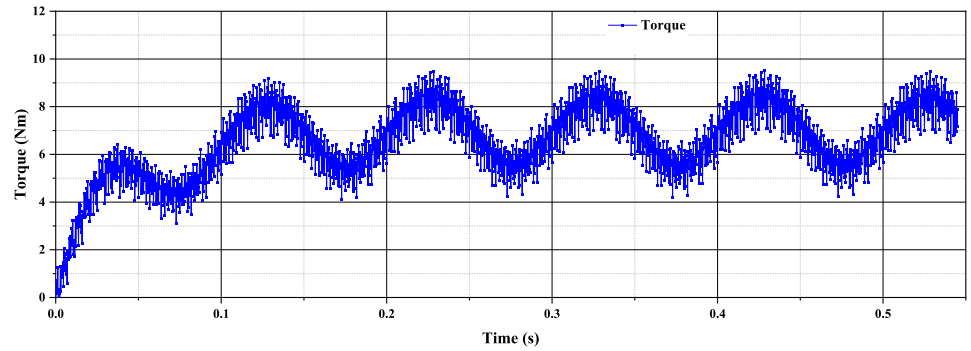

FIGURE 8. Conventional model torque.

it produces the rotor field flux without the use of brushes and slip-rings. Figure 4 represents the winding layout of the proposed design I for the armature windings ABC and XYZ. The coils for the XYZ winding are placed in 6 slots whereas

TABLE 1. Design specifications for the proposed model of the brushless wound rotor vernier machine (BI-WRVM).

PARAMETERS	UNITS	CONVENTIONAL MODEL	PROPOSED MODEL DESIGN 1/DESIGN II
ABC winding Poles	-	4	4
XYZ winding Poles	-	4	2
Excitation winding Poles	-	2	2
ABC winding Slots	-	12	21/18
XYZ winding Slots	-	12	3/6
Stator inner diamter	mm	140	140
Stator outer diameter	mm	238	238
Stator winding turns	turns/slot	90	90
Rotor field winding turns	turns/slot	36	36
Rotor excitation winding tuns	turns/slot	6	6
Rotor field poles	-	44	44
Rotor slots	-	44	44
Rotor inner diamter	mm	239	239
Rotor outer diameter	mm	300	300
XYZ winding turns	turns/slot	90	90
air Gap Length	mm	0.5	0.5
Stack length	mm	30	30
Speed	rpm		300

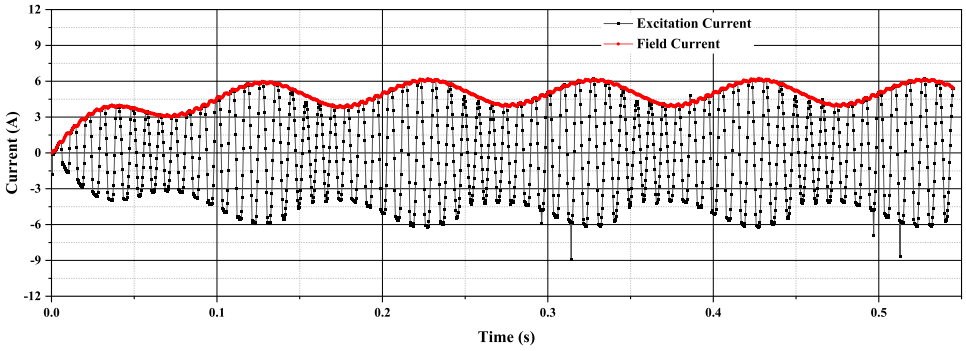

FIGURE 9. Conventional model with field and excitation currents.

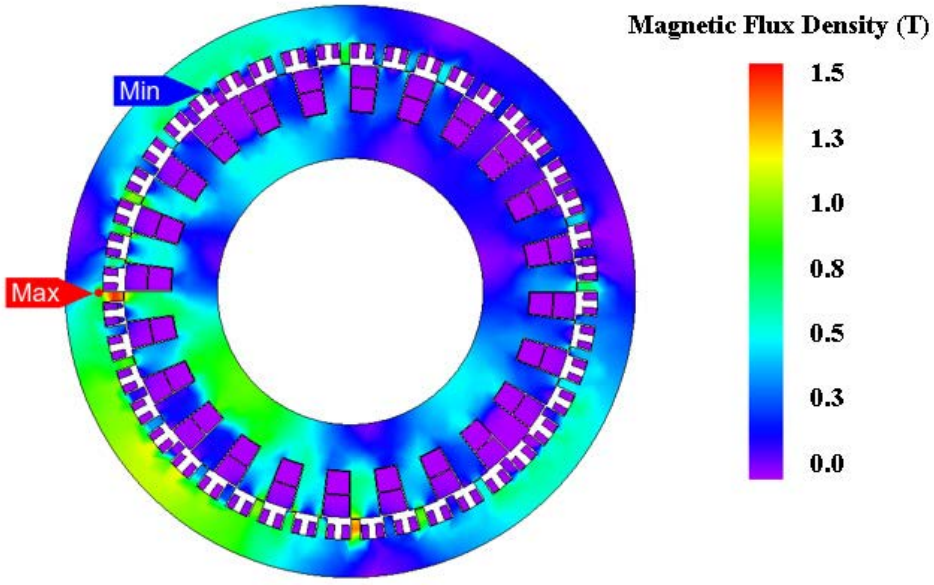

FIGURE 10. Conventional model flux density distribution.

the ABC winding is placed in 18 slots. The proposed design I consists of 3 coils for the XYZ windings and 21 coils for the ABC windings. Figure 5 represents the proposed design II of the armature winding ABC and XYZ. The proposed design II

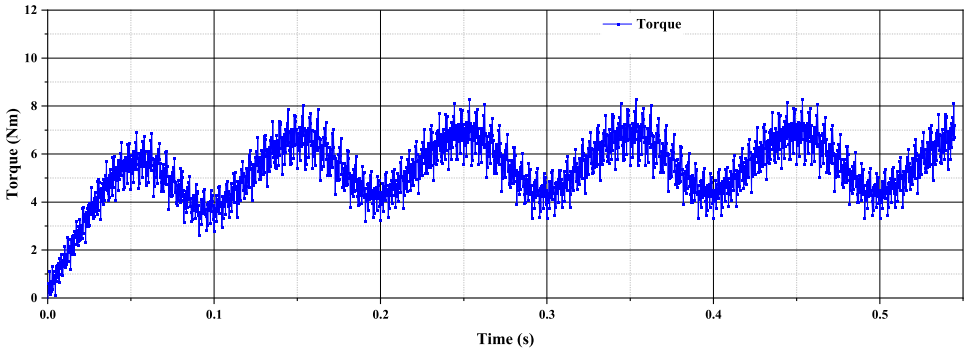

FIGURE 11. Electromagnetic torque of the proposed model design I.

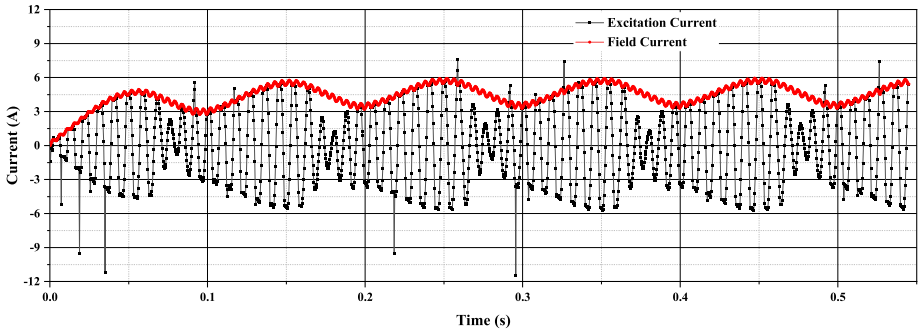

FIGURE 12. Proposed model design I field and excitation current.

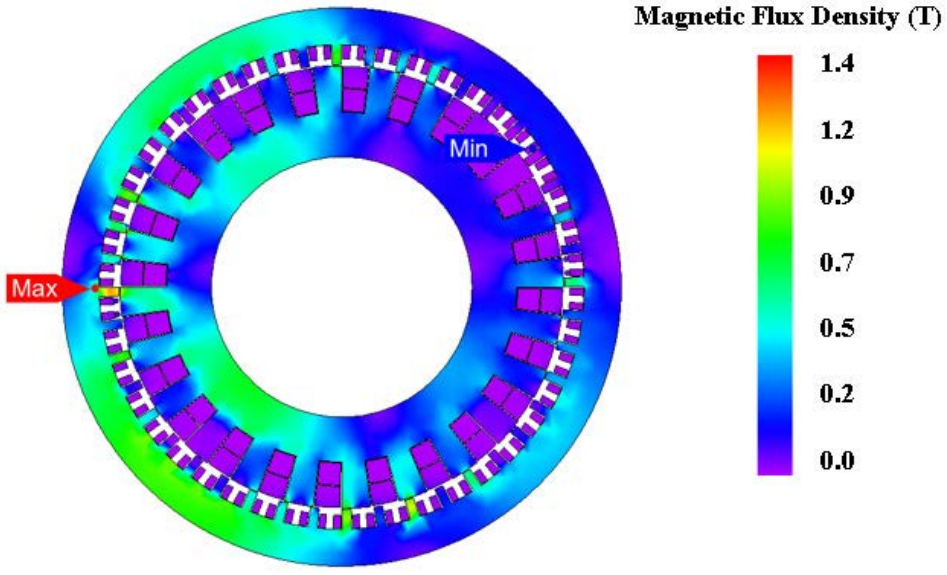

FIGURE 13. Proposed model design I flux density distribution plot.

includes 6 coils for the XYZ winding and 18 coils for the ABC windings.

A. GEOMETRICAL AND STRUCTURAL DESIGN

Table 1 displays the design parameters for the 2D model of the Bl-WRVM. Double-layer distributed winding is used in the stator's construction to produce four-pole and two-pole windings. Field and excitation windings have 44 and two poles, respectively. Figure 6 presents a 2D model of the Bl-WRVM that is used for the 2D FEA analysis. This is an outer rotor model.

The currents supplied by the inverter to the stator winding sets are given by the following equations.

$$I_A = I_X = I \cos \omega_e t$$

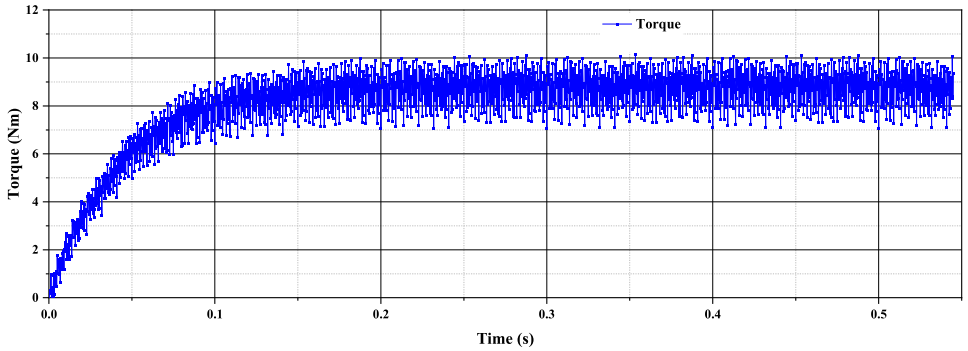

FIGURE 14. Electromagnetic torque of proposed model design II.

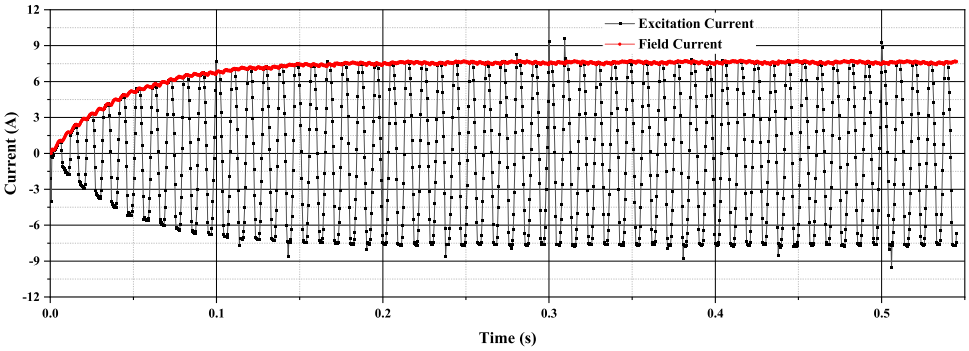

FIGURE 15. Field and excitation currents of the proposed model design II.

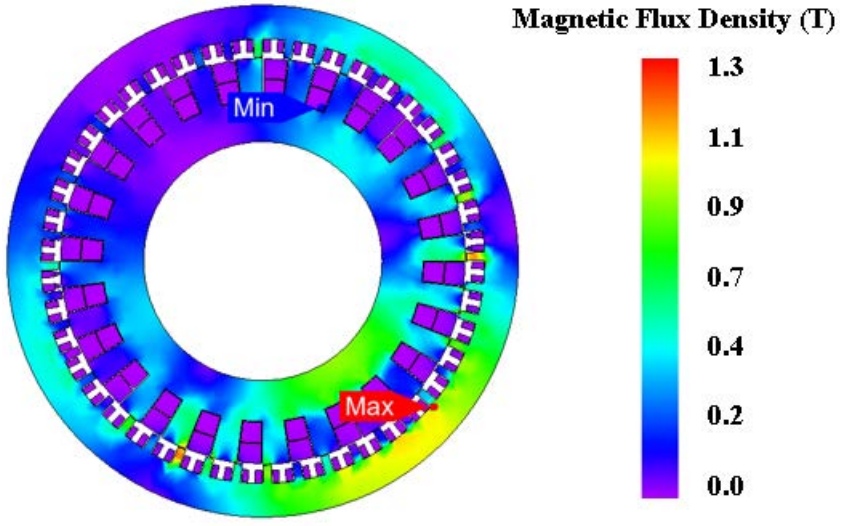

FIGURE 16. Flux density Distribution of the proposed model design II.

$$I_B = I_Y = I\cos(\omega_e t - \frac{2\pi}{3})$$
$$I_C = I_Z = I\cos(\omega_e t + \frac{2\pi}{3}) \quad (4)$$

where I signify the current amplitude and ω_e denotes angular frequency.

IV. ELECTROMAGNETIC PERFORMANCE

The 2D FEA analysis is carried out using the JMAG-Designer for the performance analysis of the brushless wound rotor vernier machine. The 2D FEA analysis shows the performance of the machine driven with both conventional and proposed brushless scheme design 1 and II in terms of excitation

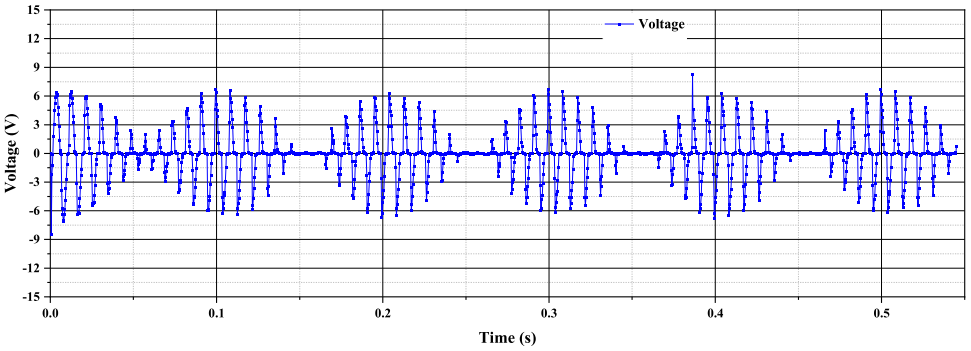

FIGURE 17. Induced voltage in the rotor excitation winding conventional model. (2.34 rms value).

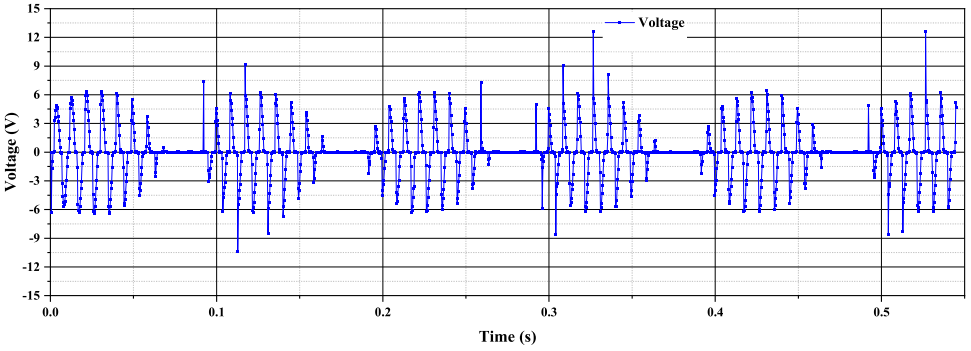

FIGURE 18. Induced voltage in the rotor excitation winding proposed model design I. (2.424 rms value).

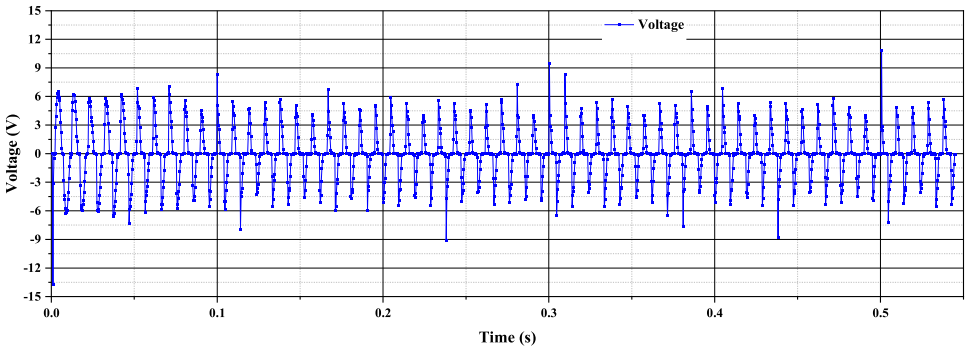

FIGURE 19. Induced voltage in the rotor excitation winding proposed model design II. (2.546 rms).

current, field current, and output electromagnetic torque. The results are compared for the conventional and proposed design 1 and II.

Figure 7 shows the current fed by the inverter to the conventional and proposed model of BL-WRVM. The peak value of the current fed by the inverter 1 is 1.3 A and the peak value of the current fed by inverter 2 is 0.66 A. Whereas the peak value of the current fed by inverter to the proposed model design 1 and II is 1 A. The peak value of 1 A is chosen to give the same average value of the current as made by the inverter 1 and 2.

Figure 8 shows the torque produced by the conventional BL-WRVM. Initially, as there is no excitation on the rotor, its torque starts from 0 Nm. Gradually it achieves its average torque of 6.516 Nm with a torque ripple of 78.26%. The high ripple is due to the harmonic content in the airgap MMF and the fluctuation in rotor field current.

Figure 9 represents the induced currents in the rotor excitation windings and the currents which are rectified by the rotating rectifier and fed to the field winding on the rotor.

Figure 10 shows the flux density distribution plot for the conventional BLWRVM. The unbalanced magnetic field on the left and right sides of the machine is due to the fact that the left side stator winding of the machine is connected to inverter I with a higher amplitude of current, while the right-side stator

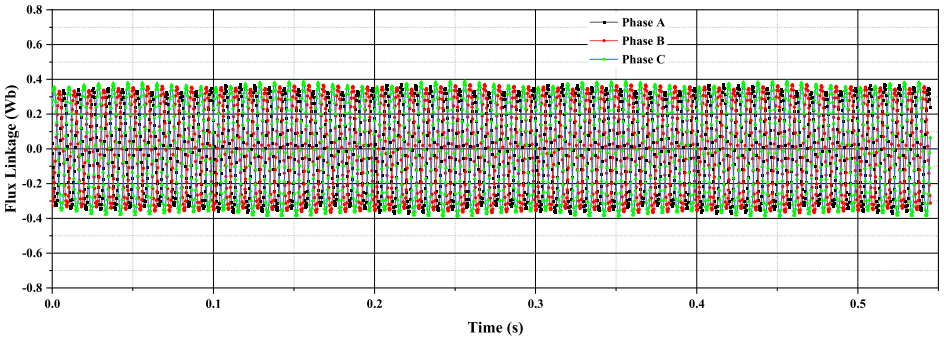

FIGURE 20. Flux linkage of the conventional model ABC winding.

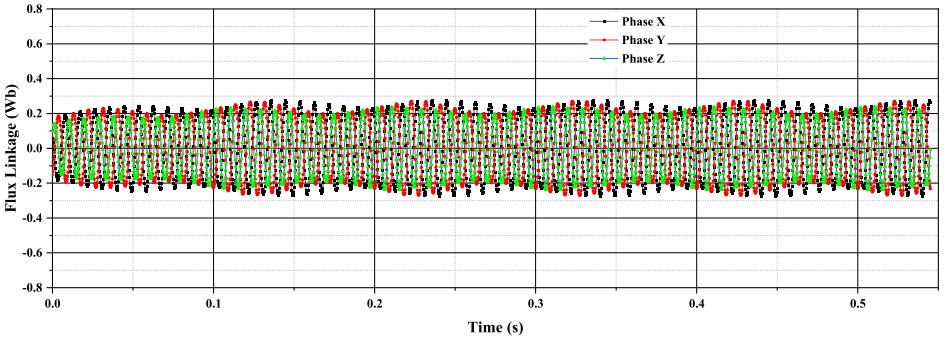

FIGURE 21. Flux linkage of the conventional model XYZ winding.

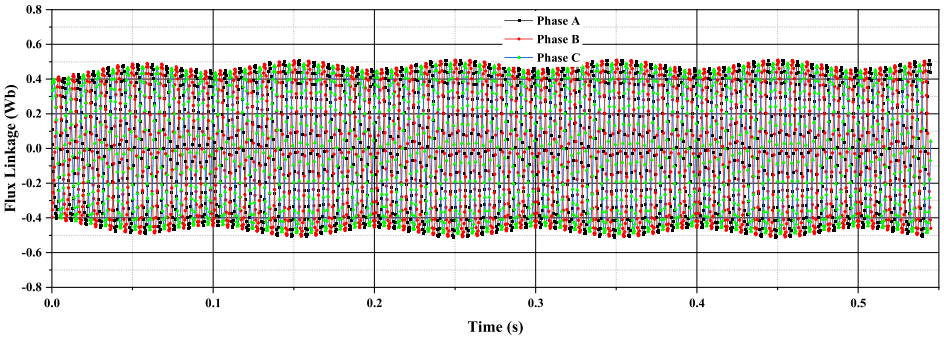

FIGURE 22. Flux linkage of the proposed model design I ABC winding.

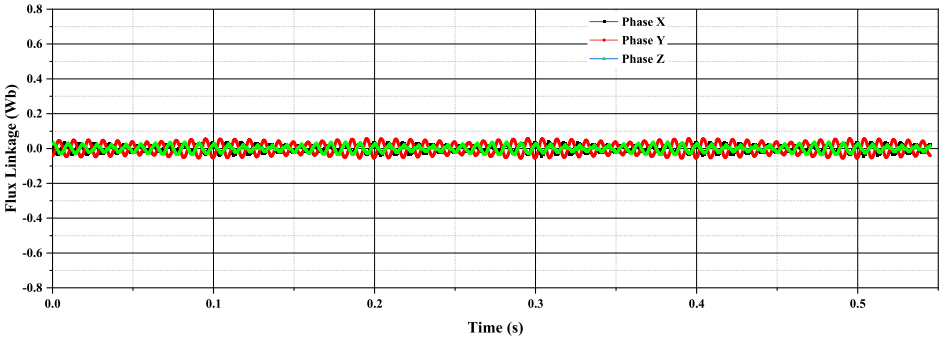

FIGURE 23. Flux linkage of the proposed model design I XYZ winding.

winding of the machine is connected to inverter II with lower amplitude of the current.

Figure 11 shows the torque generated by the proposed model design I. The average torque achieved for this

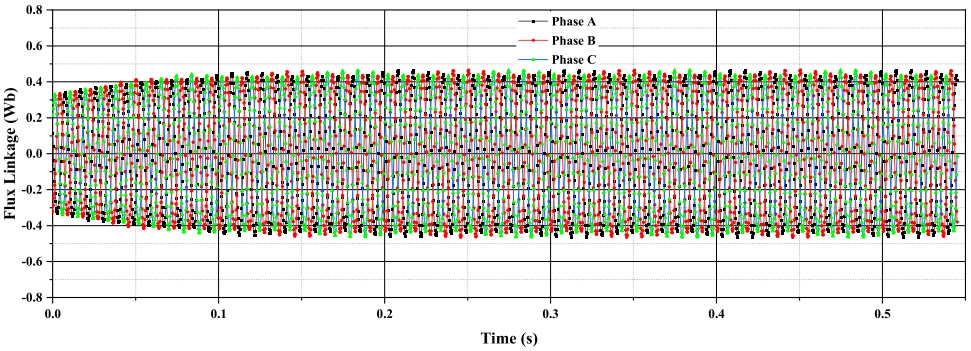

FIGURE 24. Flux linkage of the proposed model design II ABC winding.

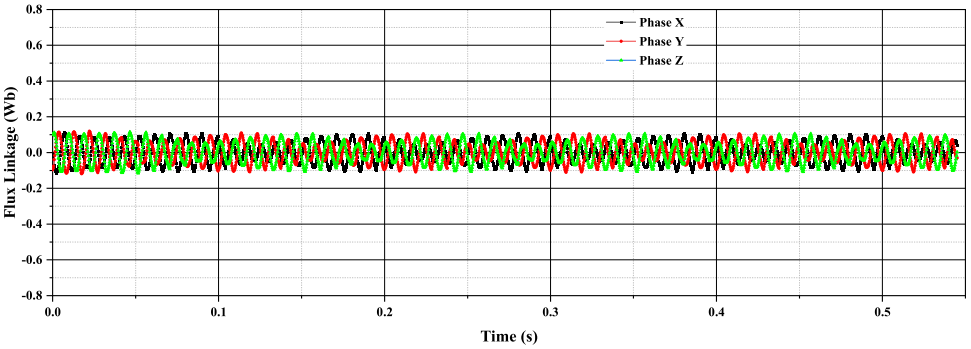

FIGURE 25. Flux linkage of the proposed model design II XYZ winding.

TABLE 2. Comparison of conventional and proposed model.

PARAMETER	UNITS	CONVENTIONAL MODEL	PROPOSED MODEL DESIGN I	PROPOSED MODEL DESIGN II
Field current	A	4.72	4.35	6.97
Excitation voltage	V	2.34	2.42	2.54
Torque	Nm	6.516	5.326	8.08
Torque Ripple	%	78.26	93.87	37.12
Efficiency	%	74.5	73	86
Power Factor	-	0.3	0.56	0.66
Torque density	Nm/m^3	2.25	1.84	2.77

configuration is 5.326 Nm and the torque ripple is 93.87 %. The performance is not very impressive as it fails to compete with the conventional model.

Figure 12 represents the induced currents in the rotor excitation windings and the currents which are rectified by the rotating rectifier and fed to the field winding on the rotor. The average value of the field current is lower than the field current developed by the conventional model. This has resulted in a decrease in electromagnetic torque.

Figure 13 represents the flux density distribution plot for the proposed model design 1. The flux density is balanced as compared to the conventional design model. Furthermore, the overall flux density distribution is lower due to the lower value of the field current.

Figure 14 shows the torque produced in the proposed model design II which is 8.08 Nm. Using the 6 slots for the XYZ winding resulted in increased torque as compared to the conventional model and proposed model design I. Furthermore, a considerable reduction in the torque ripple (37.12 %) is achieved with the proposed model design II.

Figure 15 presents the excitation and field current plot of the proposed model design II. The induced excitation current has increased and so is the field current. The increased field current is responsible for the increased electromagnetic torque production. Also, with the proposed model design II smooth field current is obtained as compared to the conventional and proposed design I.

Figure 16 shows the flux density distribution plot of the proposed model design II. The distribution plots balanced the distribution of the magnetic flux density.

Figures 17, 18, and 19 show the induced voltages in the rotor harmonic windings for the conventional proposed model I and proposed model II. It can be noted that the proposed model II shows the highest induced voltages.

Figures 20 to 25 are plotted for the flux linkages in the stator ABC and XYX windings. For ABC winding, the flux linkage is highest for proposed model II while the flux linkages in XYZ windings are reduced.

Overall performance comparison of the conventional and proposed model designs I and II in Table 2. The proposed model design II shows better performance in terms of the average torque, torque quality, power factor, torque density, and efficiency. The torque density is improved from 2.25 Nm/m^3 to 2.77 Nm/m^3 and the performance improvement in power factor is 120% whereas its efficiency is improved to 13%.

V. CONCLUSION

This paper proposes a cost-effective brushless three-phase wound rotor vernier machine. A simplified structure and topology are initially analyzed for the brushless operation of the WRVM. In this topology, two three-phase windings are mounted on the stator namely, an ABC armature winding and XYZ additional three-phase winding for excitation. To create the harmonic air gap component, the XYZ winding is configured for two-poles on a four-pole vernier machine. The working of the topology was verified by the 2D FEA. Since the machine does not use any additional inverters for a harmonic component generation or a specially built inverter for power supply, it is cost-effective compared to the conventional brushless wound rotor machines and hence can be used in automotive industries.

REFERENCES

[1] M. Bilal, J. Ikram, A. Fida, S. S. H. Bukhari, N. Haider, and J.-S. Ro, "Performance improvement of dual stator axial flux spoke type permanent magnet Vernier machine," *IEEE Access*, vol. 9, pp. 64179–64188, 2021.

[2] F. Zhao, T. A. Lipo, and B.-I. Kwon, "A novel dual-stator axial-flux spoke-type permanent magnet Vernier machine for direct-drive applications," *IEEE Trans. Magn.*, vol. 50, no. 11, pp. 1–4, Nov. 2014.

[3] I. Ahmad, J. Ikram, M. Yousuf, R. Badar, S. S. H. Bukhari, and J.-S. Ro, "Performance improvement of multi-rotor axial flux Vernier permanent magnet machine by permanent magnet shaping," *IEEE Access*, vol. 9, pp. 143188–143197, 2021.

[4] F. Wu and A. M. El-Refaie, "Permanent magnet Vernier machine: A review," *IET Electr. Power Appl.*, vol. 13, no. 2, pp. 127–137, Feb. 2019.

[5] Z. Wu, Y. Fan, Q. Zhang, and D. Gao, "Comparison and analysis of permanent magnet Vernier motors for low-noise in-wheel motor application," *IET Electr. Power Appl.*, vol. 14, no. 2, pp. 274–281, Feb. 2020.

[6] M. R. Siddiqi, T. Yazdan, J.-H. Im, Y.-K. Lee, and J. Hur, "Dual stator permanent magnet Vernier machine with yokeless rotor having single stator winding for torque density improvement," *IEEE Access*, vol. 9, pp. 151155–151166, 2021.

[7] L. Wei and T. Nakamura, "A novel dual-stator hybrid excited permanent magnet Vernier machine with Halbach-array PMs," *IEEE Trans. Magn.*, vol. 57, no. 2, pp. 1–5, Feb. 2021.

[8] F. Zhao, M. Cao, E. Tao, and L. Li, "Design and analysis of a permanent magnet Vernier machine with non-uniform tooth distribution," *Energies*, vol. 14, no. 22, p. 7816, Nov. 2021.

[9] S. Jia, R. Qu, J. Li, D. Li, and H. Lu, "Design considerations of stator DC-winding excited Vernier reluctance machines based on the magnetic gear effect," *IEEE Trans. Ind. Appl.*, vol. 53, no. 2, pp. 1028–1037, Mar. 2017.

[10] Q. U. A. Khaliq, M. Riaz, I. A. Arshad, and S. Gul, "On the performance of median-based Tukey and Tukey-EWMA charts under rational subgrouping," *Scientia Iranica*, vol. 28, no. 1, pp. 547–556, 2021.

[11] M. Riaz, Q. Khaliq, M. Abid, and I. A. Arshad, "On designing efficient sequential schemes to monitor non-normal processes," *Qual. Rel. Eng. Int.*, vol. 38, no. 1, pp. 615–634, Feb. 2022.

[12] K. D. Tran, Q.-U.-A. Khaliq, A. A. Nadi, T. H. Nguyen, and K. P. Tran, "One-sided Shewhart control charts for monitoring the ratio of two normal variables in short production runs," *J. Manuf. Processes*, vol. 69, pp. 273–289, Sep. 2021.

[13] Q. Ali, T. A. Lipo, and B.-I. Kwon, "Design and analysis of a novel brushless wound rotor synchronous machine," *IEEE Trans. Magn.*, vol. 51, no. 11, pp. 1–4, Nov. 2015.

[14] Q. Ali, A. Hussain, N. Baloch, and B. Kwon, "Design and optimization of a brushless wound-rotor Vernier machine," *Energies*, vol. 11, no. 2, p. 317, Feb. 2018.

[15] N. Baloch, S. Atiq, and B.-I. Kwon, "A wound-field pole-changing Vernier machine for electric vehicles," *IEEE Access*, vol. 8, pp. 91865–91875, 2020.

[16] G. J. Sirewal and S. S. H. Bukhari, "Cost-effective scheme for a brushless wound rotor synchronous machine," *World Electr. Vehicle J.*, vol. 12, no. 4, p. 194, Oct. 2021.